Marcus Theory: Thermodynamics CAN Control the Kinetics of Electron Transfer Reactions

ARTICLE *in* JOURNAL OF CHEMICAL EDUCATION · AUGUST 2012

Impact Factor: 1.11 · DOI: 10.1021/ed1007712

1 AUTHOR:

Todd P Silverstein
Willamette University
85 PUBLICATIONS **317** CITATIONS

SEE PROFILE

JOURNAL OF CHEMICAL EDUCATION

Article

pubs.acs.org/jchemeduc

Marcus Theory: Thermodynamics CAN Control the Kinetics of Electron Transfer Reactions

Todd P. Silverstein*

Chemistry Department, Willamette University, Salem, Oregon 97302, United States

Supporting Information

ABSTRACT: Although it is generally true that thermodynamics do not influence kinetics, this is NOT the case for electron transfer reactions in solution. Marcus Theory explains why this is so, using straightforward physical chemical principles such as transition state theory, Arrhenius' Law, and the Franck-Condon Principle. Here the background and applications of Marcus Theory are presented, with special emphasis given to biological redox reactions. Interesting conclusions that arise from the theory are also discussed. These include the nonlinear contribution of reorganization energy (λ) to the activation free energy ($\Delta G^{\ddagger}$), as well as the existence of a defined "normal range" of reaction cell potential (ΔE°): Only if ΔE° is within this range does a reaction of lower λ have a lower $\Delta G^{\ddagger}$; outside of this range, the lower-λ reaction will have the higher $\Delta G^{\ddagger}$.

KEYWORDS: *Upper-Division Undergraduate, Biochemistry, Physical Chemistry, Inorganic Chemistry, Aqueous Solution Chemistry, Bioinorganic Chemistry, Biophysical Chemistry, Catalysis, Electrochemistry, Enzymes, Kinetics, Oxidation/Reduction, Thermodynamics*

BACKGROUND

Almost all General/Introductory Chemistry textbooks and instructors at one point make the assertion that reaction thermodynamics do NOT influence kinetics: A spontaneous reaction can be slow, whereas a nonspontaneous reaction can be fast. The point of this paper is to describe a common exception to this general assertion that kinetics are independent of thermodynamics. Anderson's "90% rule" states that good rules in chemistry are correct over 90% of the time, and thus deserve their place in the teaching of General/Introductory Chemistry.[1] However, even good rules have exceptions, and as Emeric Schultz has pointed out,[1] "some of the most interesting stuff is in the 10% exceptions." These exceptions are worth mentioning, but not teaching, at the introductory level;[1] on the other hand, exceptions often include fascinating chemistry for students at the upper division undergraduate, and graduate level.

First the 90%: For most reactions there is no relationship between the standard free energy differences between reactants and products (ΔG°) on one hand, and between reactants and transition state ($\Delta G^{\ddagger}$, the activation free energy) on the other. The reasons underlying this rule are discussed in most physical chemistry texts (e.g., ref 2) under the heading "potential energy surfaces." Briefly, using simple two-dimensional parabolic potential energy curves for the reaction R → P (upper curve in Figure 1), the intersection between the reactant and the product curves gives the activation free energy (E in Figure 1). One might be tempted to predict that for a more spontaneous reaction, for example, R → P′ (lower curve, Figure 1), the activation free energy must be lower, that is, $E' < E$. However, there are two problems with this prediction: First, Figure 1 makes the unwarranted assumption that for the two reactions, *the transition states occur at identical nuclear separation distances.* Furthermore, the two-dimensionality of Figure 1 is an oversimplification. Because of the number of different interatomic distances and collision angles sampled in most reactions, a three (or more!) dimensional plot showing potential energy *contour surfaces* must be employed. Because of the complexity of these multidimensional potential energy contours, and the different nuclear separation distances of different transition states, for most reactions there is in fact no discernible relationship between $\Delta G^{\ddagger}$ and ΔG°.

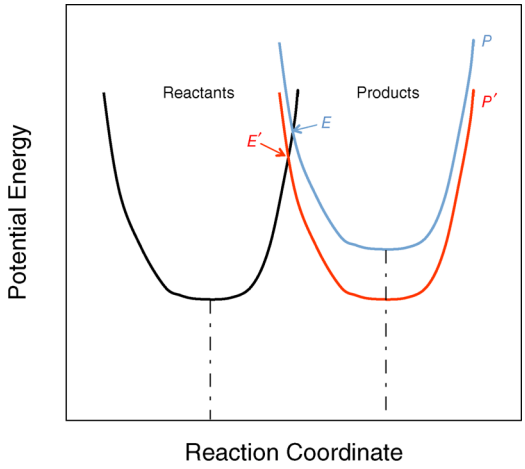

Figure 1. Potential energy curves for a nonspontaneous reaction (R → P, upper blue curve), and one that is more spontaneous (R → P′, lower red curve).

This rule works for most reactions (the 90%), but there are some notable exceptions (the 10%). For organic reactions, Hammond's postulate states that the transition state structure resembles that of the species nearest to it in free energy: In other words, all other things being equal, the free energy of activation should be higher for an endergonic reaction, and lower for an exergonic reaction.

Published: July 11, 2012

dx.doi.org/10.1021/ed1007712 | J. Chem. Educ. 2012, 89, 1159–1167

The most well-characterized exception to the thermodynamics/kinetics independence rule is the solution-phase "outer sphere" redox reaction,[3] that is, that between solvated donors and acceptors that exchange electrons. For his detailed characterization of this particular class of "exceptions to the rule", Rudolph A. Marcus won the Nobel Prize[4] in 1992. Marcus initially developed his theory to describe electron transfer between small solvated donors and acceptors, and he was later able to expand it to include electrode reactions and biological electron transfers.[5] Previous papers in *this Journal* (most published over 20 years ago) have discussed Marcus Theory in broad, general terms,[6,7] or have dealt only with the so-called "cross-relation" aspect of the theory,[8−10] or with specific experimental systems.[6,8,11] As we shall see, Marcus Theory can be explained by relatively straightforward concepts in physical chemistry (especially transition state theory and the Franck−Condon Principle). Furthermore, a number of interesting conclusions arise from the theory, including the "inverted region": redox reactions get faster as they get more spontaneous only up to a certain point; beyond this point, in the inverted region, they get slower for more negative ΔG°.

MARCUS THEORY

An outer-sphere redox reaction can be seen as a series of three steps: association, electron transfer, and dissociation (Scheme 1).

Scheme 1

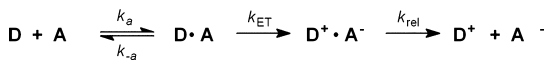

- Step 1 (association): formation of the donor−acceptor (D•A) association complex

$$K_{assocn} = k_a/k_{-a} = 1/K_{dissociation} = 1/K_d$$

- Step 2 (electron transfer): electron is passed from donor (D) to acceptor (A)[12]
- Step 3 (release): separation of the product ($D^+ \bullet A^-$) complex

All rate constants in Scheme 1 obey the Arrhenius/Eyring Laws, but in Marcus Theory, k_{ET} is especially significant:

$$k_{ET} = A_{ET} e^{-\Delta G^\ddagger/RT} \quad (1)$$

The frequency (or pre-exponential) factor, A_{ET}, is the activation-less rate constant, approached as $\Delta G^\ddagger \to 0$ (or $T \to$ infinity). As in standard Arrhenius Theory, A_{ET} gives the frequency of *effective* associations at infinite temperature.[13] Additionally for redox reactions, A_{ET} declines exponentially with the edge-to-edge separation distance (r) between donor and acceptor in the effective association complex: $A_{ET}(r) = Z\kappa(r)$, where Z has units of collision frequency, and $\kappa(r) = \kappa_0 e^{-\beta r}$ is the transmission coefficient, or the probability that electron transfer will occur once the reactant association complex reaches the transition state. The distance sensitivity, β, tends to be restricted to a narrow range (10−15 nm^{-1}),[14] and for an adiabatic reaction, that is, one with strong electronic coupling between reactants,[5,15] $\kappa \approx 1$.

Consider redox reactions involving a single donor and a series of structurally related acceptors[16] with different standard reduction potentials (E°s), and thus different cell potentials ($\Delta E^\circ = E^\circ_A - E^\circ_D$) and free energy changes ($\Delta G^\circ = -nF\Delta E^\circ$). For example, in a paper analyzed below, Candeias et al.[17] measured the kinetics of peroxidase reduction (E° = +0.88 V; see below "What is Marcus Theory Good For?") by a series of phenols with E°s ranging from +0.42 to +1.17 V, giving cell potentials of −0.29 to +0.46 V. Changes in reaction kinetics could result from differences in three distinct kinetic parameters: (1) k_a and k_{-a}, due to association (i.e., K_d); (2) A_{ET}, due to differences in donor−acceptor orientation or distance in the association complex; and (3) $\Delta G^\ddagger$. It is the latter property, the dependence of $\Delta G^\ddagger$ on ΔG° (or alternatively, ΔE°), that is explained by Marcus Theory:[18]

$$\Delta G^\ddagger = w_{rct} + \frac{\lambda}{4}\left(1 + \frac{\Delta G^{\circ\prime}}{\lambda}\right)^2 = w_{rct} + \frac{(\lambda + \Delta G^{\circ\prime})^2}{4\lambda} \quad (2)$$

where w = electrostatic work done to bring reactants (w_{rct}), or products (w_{prod}), together to form the donor−acceptor association complex, and $\Delta G^{\circ\prime} = \Delta G^\circ + w_{prod} - w_{rct}$. The parameters λ, w, ΔG°, $\Delta G^\ddagger$ are all energy terms with units of kJ/mol (or kcal/mol). Often in the literature, the assumption is made that $w_{prod} \approx w_{rct}$, in which case $\Delta G^{\circ\prime} \approx \Delta G^\circ = -nF\Delta E^\circ$, and eq 2 can be written as

$$\Delta G^\ddagger = w_{rct} + \frac{nF(\lambda - \Delta E^\circ)^2}{4\lambda} \quad (3)$$

Here λ is in eV and ΔE° is in V; multiplying by nF converts to kJ/mol.

Equation 2 shows that for outer sphere redox reactions there *is* a mathematical relationship between $\Delta G^\ddagger$ and ΔG°. The reason why this is so will be discussed below in the "Quantum Mechanical Explanation" section. Suffice it to say here that because the electron is so light and transfers so quickly, nuclear separation distances remain constant as the electron is transferred, and Figure 1 becomes a reasonable approximation of potential energy changes during the reaction.

Equation 2 introduces an important new component of $\Delta G^\ddagger$, the "reorganization" energy, λ. Marcus describes λ as the energy input necessary to alter the structure of solvated reactants to match that of solvated products, *before* electron transfer takes place.[4,5] It can be broken up into an inner shell component (λ_{in}) involving changes in bond lengths and angles, and an outer shell component (λ_{out}) involving reorientation of the surrounding solvent shell. The two components are always positive, and are additive: $\lambda = \lambda_{in} + \lambda_{out}$.

Equations 1−3 show that for outer sphere redox reactions, reaction thermodynamics (ΔG° or ΔE°) really do influence reaction kinetics. Figure 2 depicts how $\Delta G^\ddagger$ (solid, black curve) varies with cell potential (ΔE°), for λ = 0.5 eV and w_{rct} = 5 kJ/mol.

Because eq 3 is a second order polynomial in ΔE°, the $\Delta G^\ddagger$ (solid) curve is a parabola; its minimum occurs at ΔE° = 0.5 eV = λ, and $\Delta G^\ddagger_{min} = w_{rct}$. At this point, the free energy supplied by the spontaneous reaction is equal and opposite to the reorganization energy; the second term in eq 3 disappears here (i.e., $\lambda - \Delta E^\circ = 0$), so only w_{rct} contributes to $\Delta G^\ddagger$.

Two inferences can be drawn from the curves in Figure 2: The left side shows that as the redox reaction gets less spontaneous (i.e., $\Delta E^\circ < \lambda$) the reaction gets slower (higher $\Delta G^\ddagger$), which makes some intuitive sense (even though we implore our students NOT to draw conclusions like this!). By the same token though, the right side of the parabola tells us that as the redox reaction gets *more* spontaneous (i.e., $\Delta E^\circ > \lambda$)

dx.doi.org/10.1021/ed1007712 | J. Chem. Educ. 2012, 89, 1159−1167

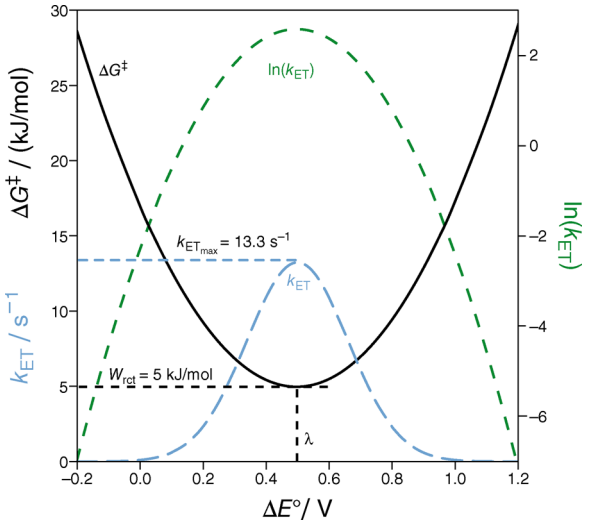

Figure 2. Marcus Theory predictions for the variation with cell potential (ΔE°) of activation free energy ($\Delta G^\ddagger$, solid curve, left scale, from eq 3); k_{ET}, long dashed curve, left scale, from eq 1 and 3; and $\ln(k_{ET})$, short dashed curve, right scale. Parameter values used are: λ = 0.5 eV, w_{rct} = 5 kJ/mol, T = 25 °C, and A_{ET} = 100 s^{-1}. At ΔE° = 0.5 eV = λ, $\Delta G^\ddagger_{min} = w_{rct}$, and $k_{ET}(max) = 13.3 = A_{ET}\ e^{-w(rct)/RT}$.

the reaction also gets slower (higher $\Delta G^\ddagger$). Marcus refers to this right side of the parabola as the "inverted region".[4]

Using the same parameter values (λ = 0.5 eV and w_{rct} = 5 kJ/mol) plus T = 25 °C and A_{ET} = 100 s^{-1}, we see that the k_{ET} vs ΔE° plot gives the bell-shaped blue (long dashes) curve. As with the $\Delta G^\ddagger$ minimum in Figure 2, the maximum value of k_{ET} occurs at ΔE° = 0.5 eV = λ. Interestingly, the k_{ET} vs ΔE° blue curve resembles a condensed phase UV–vis absorbance peak: There is a particular energy that yields the highest y-value, with higher *or* lower energy values giving successively lower y-values. As with absorbance, the shape of the curve is explained by quantum mechanical considerations (discussed below).

It is worth mentioning here that Marcus Theory analyses are often depicted with $\ln(k)$ vs ΔE° (or ΔG°) curves (Figure 2, short dashed curve). Such semilog plots have advantages (they stretch apart small y-values and compress large ones together), but they tend to give undue weight in any fitting procedure to the lowest, most error-prone values.

QUANTUM MECHANICAL EXPLANATION

Marcus explains the inverted region on the basis of the Franck–Condon Principle and corresponding potential energy diagrams. Because the electron is such a light particle, the Franck–Condon Principle applies even to "weak overlap" electron transfers.[5] During the fast electron transfer process, nuclei have no time to shift position, thus the electron transfer occurs mainly at or near the intersection of the reactant and product potential energy curves[19] as depicted in Figure 3, right. It is here that the overlap of wave functions for reactant and product potential energy curves is maximal. In Figure 3 this intersection point is marked as g_1, which also denotes the position and energy of the transition state. In the endergonic reaction depicted in Figure 3, for a reactant molecule to cross from the R potential energy curve to P_1 (red dotted line in Figure 3, right), the highest energy point it passes through is g_1. In this case, the free energy of activation is $g_1 - g_R = \Delta G^\ddagger_1$, which exceeds ΔG°_1.

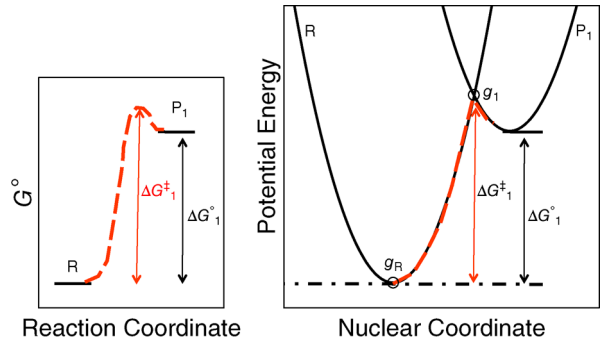

Figure 3. Reaction coordinate (*left*) and potential energy (*right*) diagrams for the endergonic reaction R → P_1. The red dotted line follows the trajectory for reactants converting to products; $\Delta G^\ddagger_1 = g_1 - g_R > \Delta G^\circ$.

In Figure 4, the endergonic R → P_1 reaction from Figure 3 is compared to more spontaneous reactions. For the reaction R

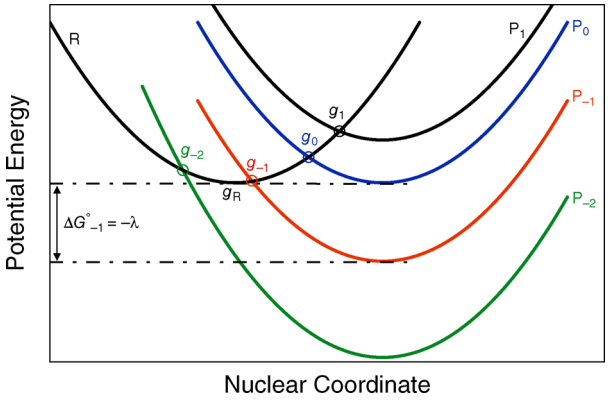

Figure 4. Potential energy diagrams for conversion of reactants R to four different products: P_1 (black), less stable than R (as in Figure 3); P_0 (blue), ΔG° = 0; P_{-1} (red), exergonic with $\Delta G^\ddagger_{-1} \approx 0$ ($\Delta G^\circ_{-1} = -\lambda$); and P_{-2} (green), more stable than P_{-1}. Based on Figures 1, 3, and 5 of ref 5.

→ P_0 (Figure 4, blue curve), ΔG° = 0, and $\Delta G^\ddagger_0 = g_0 - g_R$. Because g_0 is lower than g_1, $\Delta G^\ddagger_0 < \Delta G^\ddagger_1$, and the more spontaneous reaction (R → P_o) is faster.

The exergonic reaction R → P_{-1} (Figure 4, red curve) is a special case: The P_{-1} curve crosses the R curve near its lowest point (g_{-1} is only slightly above g_R). This reaction is nearly barrierless ($\Delta G^\ddagger_{-1} \approx 0$), and it reacts at close to the diffusion-controlled limiting rate: $k \approx A_{ET}$. The rate is maximal because the P_{-1} curve intersects the R curve near its most highly populated (i.e., lowest energy) point, so the crossing probability is highest. Nevertheless, even for this optimal reaction, an association complex must still form, and reactant and solvent molecules must still reorganize themselves to reach and cross through the transition state on the way to products. Hence the reorganization energy is not zero. From eq 2 it follows that $\Delta G^\ddagger_{-1}$ is minimal because $\Delta G^\circ + \lambda \approx 0$. One way to envision this situation is that the free energy released as the reaction proceeds ($\Delta G^\circ \approx -\lambda$) is "invested" in the reorganization process, such that the activation free energy is minimized.

Considering the three reactions discussed above, R → P_1 vs P_0 vs P_{-1}, as ΔG° gets more negative, $\Delta G^\ddagger$ decreases and the reaction goes faster. This Marcus Theory prediction is observed on the left side of the curves in Figure 2. However, $\Delta G^\circ = -\lambda$ is

dx.doi.org/10.1021/ed1007712 | J. Chem. Educ. 2012, 89, 1159–1167

the optimal point: Any reactions more spontaneous than this actually go slower. As we saw in our discussion of Figure 2 above, this situation can be likened to a condensed phase UV–vis absorbance peak: higher energy incident photons lead to higher absorbances only up to a certain point, that point being the energy difference between the ground and excited states. Incident photons above this energy are absorbed *less*. Analogously, as reaction free energies decrease below $-\lambda$, reactions get slower.

This effect can be seen by comparing the green P_{-2} curve to the red P_{-1} curve in Figure 4. Clearly, ΔG° ($R \rightarrow P_{-2}$) is more negative than ΔG° ($R \rightarrow P_{-1}$); on the other hand, because g_{-2} is *higher* than g_{-1}, $\Delta G^\ddagger_{-2}$ exceeds $\Delta G^\ddagger_{-1}$, and the $R \rightarrow P_{-2}$ reaction is slower. Thus decreases in ΔG° below $-\lambda$ feature higher $\Delta G^\ddagger$, as predicted by the Marcus Theory "inverted region" and observed on the right side of the curves in Figure 2.

REORGANIZATION ENERGY

As discussed above, the reorganization energy (λ) is generally described as the energy necessary to reorganize reactant bonds and surrounding solvent to match those found in the product. Using simple parabolas for the reactant and product potential energy curves ($PE = kx^2$), it can be shown that the reorganization energy is identical to $k\Delta r^2$, where Δr is the nuclear coordinate separation distance between reactants and products (see Supporting Information B). This lends a quantum mechanical meaning to the above description, namely, that λ is the energy input necessary to move reactants along their parabolic potential energy curve to a nuclear coordinate separation equal to Δr, corresponding to the most stable configuration for the products.

Another important point to make is that the reorganization energy contributes to the activation free energy, but not in a simple, additive way. As we shall see below, authors often infer that as λ increases, $\Delta G^\ddagger$ increases; however, this is not always the case. In fact, from eq 3 it is clear that for large values of λ ($\lambda \gg \Delta E^\circ$), $\Delta G^\ddagger$ increases linearly with λ, but for small values of λ ($\lambda \ll |\Delta E^\circ|$), $\Delta G^\ddagger$ is *inversely* proportional to λ (Figure 5). Thus for $\lambda \geq |\Delta E^\circ|$, as λ increases, $\Delta G^\ddagger$ rises (and k_{ET} declines); this is the situation envisioned by many authors. However, for $\lambda \leq |\Delta E^\circ|$, as λ *decreases,* $\Delta G^\ddagger$ rises (and k_{ET} declines). Hence to predict correctly the effect on $\Delta G^\ddagger$ of a change in λ, one must know where both reorganization energies lie relative to the cell potential of the reaction.[20] Although the significance of the Marcus Theory inverted region is widely recognized, this mathematical complexity in how λ impacts $\Delta G^\ddagger$ is often overlooked, and is worth further clarification.

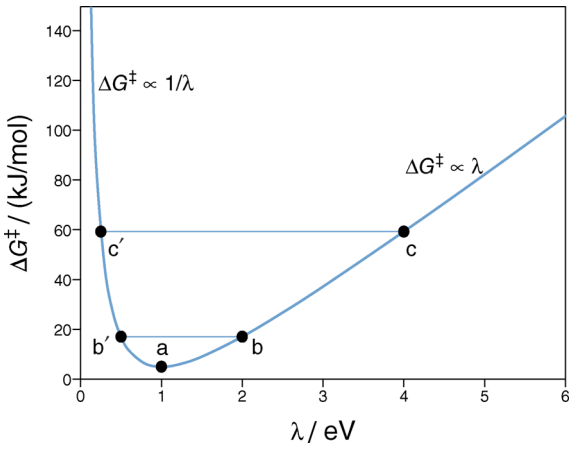

Figure 5. Dependence of activation free energy ($\Delta G^\ddagger$) on reorganization energy (λ), from Marcus Theory, eq 3. Parameter values used are: $\Delta E^\circ = +1.0$ V, $w_{rct} = 5$ kJ/mol. $\Delta G^\ddagger_{min} = w_{rct}$, at $\lambda = 1.0$ V $= \Delta E^\circ$ (point *a*). Points *b* and *b*′ ($\lambda = 2$ eV, 0.5 eV, respectively) have identical $\Delta G^\ddagger$ values, as do points *c* and *c*′ ($\lambda = 4$ eV, 0.25 eV, respectively). From eq 3, $\Delta G^\ddagger(\lambda_{low}) = \Delta G^\ddagger(\lambda_{high})$ when $\lambda_{low} = \Delta E^{\circ 2}/\lambda_{high}$.

Figure 6 uses a specific comparison to view the complex mathematical relationship between λ and $\Delta G^\ddagger$: Here we plot

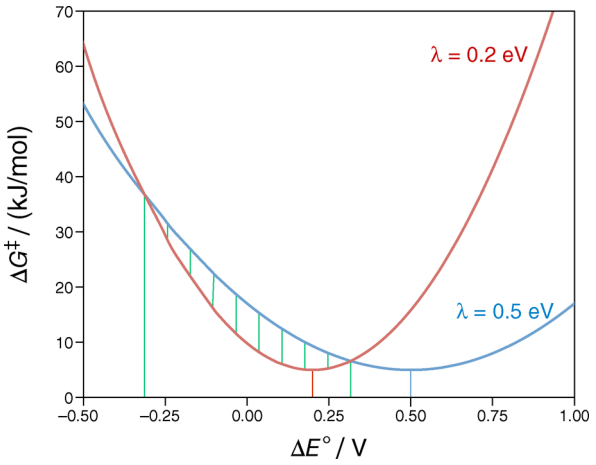

Figure 6. Marcus Theory predictions for the variation of activation free energy ($\Delta G^\ddagger$) with cell potential (ΔE°), based on eq 3. $\lambda = 0.5$ eV (blue curve) or 0.2 eV (red curve); $w_{rct} = 5$ kJ/mol; $T = 25$ °C.

$\Delta G^\ddagger$ as a function of ΔE° for two different reactions, one with $\lambda = 0.5$ eV (blue curve, as in Figure 2) and another with $\lambda = 0.2$ eV (red curve). We can see that the small green-shaded region is the only region in which the red curve (lower $\lambda = 0.2$ eV) features an activation free energy that is lower than that for the blue curve (higher $\lambda = 0.5$ eV). Outside of this "normal" region, the opposite is the case: the red curve has a higher $\Delta G^\ddagger$ than the blue curve. The green-shaded "normal" region stretches from $\Delta E^\circ = -0.32$ to $+0.32$ V. In fact, it can be shown[20] from eq 3 that this region is bounded by $\Delta E^\circ = \pm(\lambda_{low}\lambda_{high})^{1/2}$.

Similarly, Figure 7 plots k_{ET} as a function of ΔE° for both $\lambda = 0.5$ eV (blue curve, as in Figure 2) and for $\lambda = 0.2$ eV (red curve). Again, within the green-shaded "normal" region bounded by $\Delta E^\circ = \pm 0.32$ V ($= \pm (\lambda_{low}\lambda_{high})^{1/2}$),[21] k_{ET} is higher for the red curve (lower λ, 0.2 eV). Outside of this region, the red curve (lower λ) has a lower k_{ET} than the blue curve. This notion of a "normal" range of cell potentials, bounded by $\pm (\lambda_{low}\lambda_{high})^{1/2}$, is an important aspect of Marcus Theory: Within this range, the high-λ reaction is slower, but outside of this range, the high-λ reaction is faster.

We also see from Figure 7 that the reorganization energy, λ, not only sets the location of the maximum on the cell potential axis ($\Delta E^\circ = \lambda$), but it also controls the width of the k_{ET} vs ΔE° peak. Specifically, the lower-λ red peak is narrower than the higher-λ blue peak. In fact, from eq 3 it can be derived that the width of the k_{ET} vs ΔE° peak at half-height, $\Delta w_{1/2}$, is proportional to $\sqrt{\lambda}$.[22] The fact that λ figures into both the location and the width of the k_{ET} vs ΔE° peak puts an important constraint on fitting experimental results.

dx.doi.org/10.1021/ed1007712 | J. Chem. Educ. 2012, 89, 1159–1167

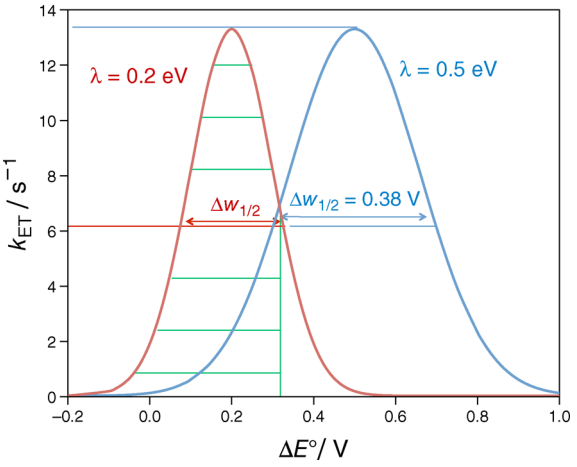

Figure 7. Marcus Theory predictions for the variation of k_{ET} with cell potential (ΔE°), based on eqs 1 and 3; λ = 0.5 eV (blue curve) or 0.2 eV (red curve); A_{ET} = 100 s^{-1}; w_{rct} = 5 kJ/mol; T = 25 °C; for the blue curve, $\Delta w_{1/2}$ = 0.38 V = (0.534 $V^{1/2}$)·(0.5 V)$^{1/2}$ (see note in ref 22).

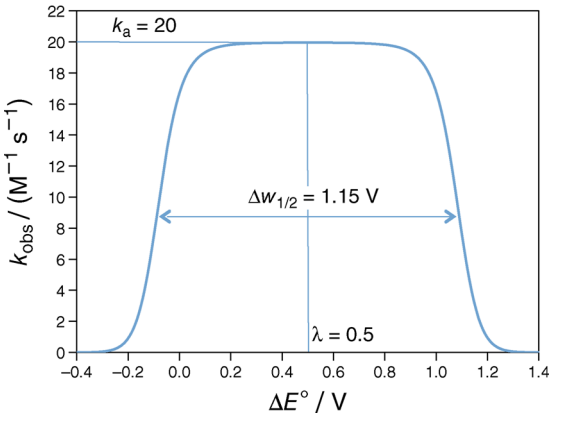

Figure 8. Association = rate-determining step; Marcus Theory prediction for the varia-tion of k_{obs} as a function of cell potential. λ = 0.5 eV; k_a = 20 M^{-1} s^{-1}; k_{-a} = 0.02 s^{-1}; A_{ET} = 100 s^{-1}; w_{rct} = 5 kJ/mol; and T = 25 °C. Note the wide, flat-topped peak: $k_{obs,max}$ saturates at k_a = 20 M^{-1} s^{-1}. From note in ref 22, $\Delta w_{1/2}$ = 1.15 V = $\Delta w_{1/2}$ = $4(\lambda\cdot((-w_{rct} + RT\ \ln(A_{ET}/k_{-a}))/(nF))^{1/2})$.

RATE-DETERMINING STEP: ASSOCIATION VS ELECTRON TRANSFER

In Scheme 1 above, we saw that the complete redox reaction comprises three steps, each with its associated rate constants. The observed reaction rate with its overall rate constant, k_{obs}, in turn depends on rate constants for all three steps: association (k_a/k_{-a}), electron transfer (k_{ET}), and separation (k_{rel}). Using the steady state approximation (i.e., assume that k_{ET} is the rate-determing step; see Supporting Information C for derivation),

$$k_{obs} = k_{ET}k_a/(k_{ET} + k_{-a}) = k_a/(1 + k_{-a}/k_{ET}) \quad (4)$$

Given the Arrhenius/Eyring equation (eq 1: $k_{ET} = A_{ET}e^{-\Delta G^{\ddagger}/RT}$) and the Marcus equation (eq 3), eq 4 has a total of three fittable parameters: k_a, k_{-a}/A_{ET}, and λ. Typically, either association or electron transfer will be the rate-determining step: For reactions in which **electron transfer is rate-limiting**, that is, $k_{ET} \ll k_{-a}$, eqs 1 and 4 reduce to eq 5

$$k_{obs} \approx k_{ET}/K_d = (A_{ET}/K_d)e^{-\Delta G^{\ddagger}/RT} \quad (5)$$

which has only two fittable parameters: (A_{ET}/K_d) and λ, the latter arising from using eq 3 to express $\Delta G^{\ddagger}$. In this case, plots of k_{obs} vs ΔE° feature sharp peaks resembling Figure 2 and 5b, with the only difference being that k_{obs} is a second order rate constant, with units of M^{-1} s^{-1} (as opposed to k_{ET} which is first order).

The opposite case is more complex, but where **association is rate-limiting** (i.e., $k_{ET} \gg k_{-a}$), eq 4 reduces to: $\boldsymbol{k_{obs} \approx k_a}$. On the other hand, k_{ET} declines rapidly for ΔE° values far from λ, to the point where ET inevitably becomes rate-limiting. This yields a k_{obs} vs ΔE° curve which is wide and flat-topped (Figure 8): For $\Delta E^\circ \approx \lambda$, k_{obs} saturates at k_a, but for ΔE° further from λ, k_{obs} declines to zero. An important implication here is that one can tell from the shape of the k_{obs} vs ΔE° curve whether the rate-limiting step is association (wide flat-topped curve) or electron transfer (narrow sharp peak).

WHAT IS MARCUS THEORY GOOD FOR?

Marcus Theory has been used successfully to predict rate constants and solvent effects for simple outer-sphere redox reactions[4,5] such as the so-called "cross-reactions" between inorganic redox couples ($A_{ox} + B_{red} \rightarrow A_{red} + B_{ox}$). Marcus and others have also expanded the theory to include electrochemical reactions at solid electrodes.[4,5,23,24]

Another area where Marcus Theory is having an ongoing impact is in the field of biological electron transfer.[4,5] The theory has been applied to a number of redox enzymes, including peroxidase,[25−31] laccase,[30−32] glucose oxidase,[33−37] cytochromes,[5] and photosynthetic reaction centers.[4,5,38] The general idea in these studies is to fit k_{obs} (or k_{cat}/K_m) vs ΔE° data to eqs 1−3 and obtain best-fit values for λ and A_{ET}/K_d. A range of cell potentials is usually obtained by using a series of structurally related substrates; depending on the enzyme these could be electron donors or acceptors. Less commonly, the same substrate can be used with a series of mutant enzymes of varying redox potential.

Marcus Theory analysis can answer a number of interesting questions regarding redox enzyme kinetics. Here I summarize recent results from just two redox enzymes, peroxidase and glucose oxidase. The Fe^{3+}-heme in peroxidase is initially oxidized by peroxide in a two-electron process (k_1), and then rereduced by two substrate molecules in a sequence of two consecutive one-electron steps. The first of these one-electron steps (k_2, reduction of Fe^{4+}-heme$^{\cdot+}$ to Fe^{4+}-heme) is always significantly faster than the second step (k_3, reduction of Fe^{4+}-heme to Fe^{3+}-heme). Folkes and Candeias[25] set out to answer this question: Is k_2 faster than k_3 because of more optimal substrate binding ($k_a/k_{-a} = 1/K_d$), orientation/distance (A_{ET}), or reorganization energy (λ)? Using horseradish peroxidase at pH 7 and a series of phenol reductants, they found (Figure 9 and Table 1) that the reorganization energy was ≈0.5 eV for both k_2 and k_3 (range: 0.35−0.5 eV). This is perhaps not surprising, as the substrate is identical in the two steps, and only the redox state of the heme is different. In fact, studies have shown no detectable structural changes occur near the heme upon reduction of Fe^{4+}-heme$^{\cdot+}$ to Fe^{4+}-heme.[39,40] On the other hand, A_{ET}/K_d was over 10-fold lower for k_3 relative to k_2 (Table 1); this can be seen in Figure 9 in the much smaller peak height of k_3. Thus the k_2/first heme reduction step (from Fe^{4+}-heme$^{\cdot+}$ to Fe^{4+}-heme) causes a conformational change at the substrate binding site or the active site: (a) At the substrate binding site, a decrease in binding affinity would raise K_d (and lower k_3); (b) at the active site, rotating the substrate or heme into a suboptimal orientation would lower A_{ET} (thus lowering k_3);

dx.doi.org/10.1021/ed1007712 | J. Chem. Educ. 2012, 89, 1159−1167

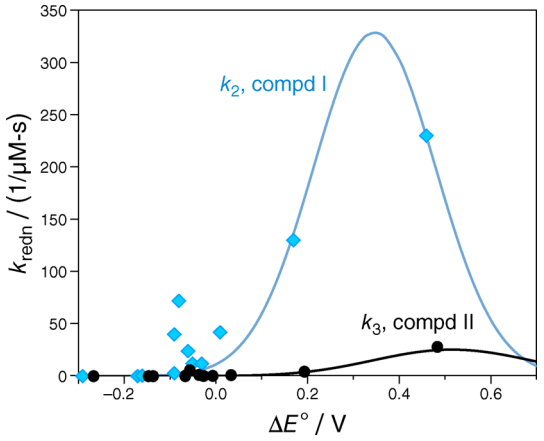

Figure 9. Horseradish peroxidase reduction by phenols and indoles. Phenol substrates, pH 7 (data from ref 25): first enzyme reduction step (compound I reduction, k_2), blue diamonds; second enzyme (compound II) reduction, k_3, black circles. Data are fit to eqs 3 and 5, assuming electron transfer is rate-limiting. Solid lines use best-fit values for λ and A_{ET}/K_d from nonlinear regression (Kaleidagraph) listed in Table 1. Although three-parameter fits (λ, k_a, and A_{ET}/k_{-a}) to eqs 1, 3, and 4 are marginally better, P-values for the fit parameters (obtained from PeakFit) show that use of the model is not statistically justified by the data points, which are too few and too scattered.

alternatively, (c) increasing the distance between substrate and heme would also lower A_{ET}, however, NMR data suggest[41] that the heme-substrate distance in peroxidase is consistently about 10 Å.

Candeias et al. also studied[27,28] the kinetics of the first enzyme reduction step (k_2) using phenols at pH 7, and indoles at pH 7 and pH 5. Enzyme reduction at pH 7 is generally slower using indole substrates relative to phenols, except at $\Delta E^\circ \approx +30$ mV. The indoles at pH 7 (Supporting Information, Figure S1a and Table 1) had a surprisingly low reorganization energy (0.0108 ± 0.0009 eV), showing that the indole and the enzyme heme are bound "in a geometry ideal for electron transfer [similar to] optimized systems such as the bacterial photosynthetic reaction center.[28]" Note that as pointed out above, a low reorganization energy does not necessarily mean fast electron transfer. In fact, when comparing phenols vs indoles at pH 7 (λ = 0.35 vs 0.01 eV, respectively), the "normal" range[20] is ΔE° between +0.04 and −0.04 V. Since all but one of the indole points lie *outside* of this range, at pH 7 the 45-fold lower reorganization energy of indoles (relative to phenols) causes the reaction rate to be *slower*, not faster. Of course, the 6-fold lower value of A_{ET}/K_d for indoles (relative to phenols, Table 1) also contributes to reaction sluggishness.

For indoles, over much of the cell potential range enzyme reduction is faster at pH 5 compared to pH 7 (Supporting Information, Figure S1a): A_{ET}/K_d (which is 8-fold higher at pH 5) accounts for some but not all of this effect. At pH 5, the indole reorganization energy is 0.049 ± 0.006 eV (Table 1), almost five times higher than at pH 7. Because the "normal" range comparing these two reactions stretches from ΔE° = +0.02 to −0.02 V, most of the data lie *outside* of this range. As with the previous comparison above, the *higher* λ at pH 5 helps to account for the *higher* rate constants and *faster* reaction.

A few comments are in order here concerning the peroxidase results discussed above. First of all, there is an interesting difference between the phenols k_2 vs k_3 comparison (Figure 9) and the phenols vs indoles k_2 comparison (Supporting Information, Figure S1a). For phenols at pH 7, k_2 is consistently higher than k_3, over the entire range of cell potentials tested, even at very low ΔE° (Figure 10). On the

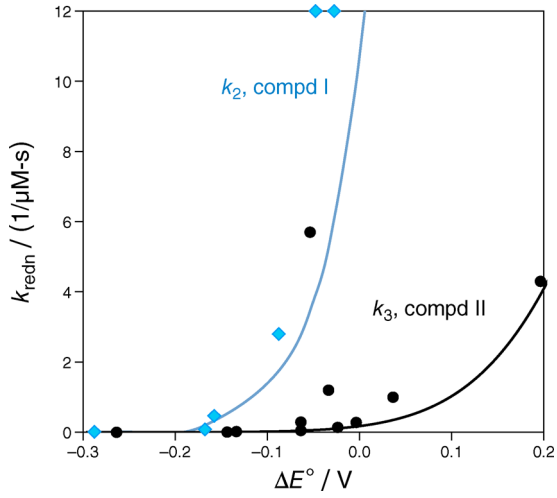

Figure 10. A subset of data from Figure 9.

Table 1. Fitted Kinetic Parameters for the Reduction of Horseradish Peroxidase (HRP) by Phenols or Indoles, at pH 7 or 5[a]

	λ (eV)	A_{ET}/K_d ($\mu M^{-1}s^{-1}$)	Relative rate	ΔE° range (V)	"Normal" range (V)	R^2
HRP k_3, phenols, pH 7, (ref 7)	0.50 ± 0.05	28.2 ± 2.2	Low	−0.3 to +0.5		0.95
From semilog slope:	0.44 ± 0.23	29 ± 22				0.90
HRP k_2, phenols, pH 7, (ref 7)	0.346 ± 0.016	**330** ± 40	High	−0.3 to +0.5	±0.47	0.85
From semilog slope:	0.6 ± 0.3					0.95
HRP k_2, indoles, pH 7, (ref 9)	**0.0108** ± 0.0009	**52** ± 4	Low[43]	−0.1 to +0.07	±0.04	0.993
From semilog slope:	0.012 ± 0.005	36 ± 12				0.90
HRP k_2, indoles, pH 5, (ref 10)	**0.049** ± 0.006[44]	**430** ± 40[44]	Moderate[45]	−0.2 to +0.03	±0.02	0.999
From semilog slope:	0.052 ± 0.024	500 ± 400				0.97

[a]For peroxidase reduction, k_2 refers to the one-electron reduction of compound I (Fe^{4+}-heme$^{\cdot+}$) to compound II, and k_3 to the one-electron reduction of compound II (Fe^{4+}-heme) to resting enzyme (Fe^{3+}-heme). **Bolded** parameters (A_{ET}/K_d, λ, or both) are responsible for the differences in relative rates. Data from Figure 9 and Supporting Information, Figure S1a are fit to eq 3 and 5, assuming $w_{rct} \approx 0$ and electron transfer is rate-limiting (i.e., $A_{ET} \ll k_{-a}$).[42] Two-parameter fits (λ and A_{ET}/K_d) are obtained by nonlinear regression (Kaleidagraph), and judged to be statistically significant by P-values from PeakFit. Values for λ listed in the "from semi-log slope" row are obtained from the slopes of the lines in Figure 11 and Supporting Information, Figure S1b, using eq 8. A_{ET}/K_d values in this row are averages of values obtained by using eq 3 and 5, applied to each (cell potential, k_{obs}) data point in the linear range, along with λ obtained from the linear range slopes in Figure 11 and Supporting Information, Figure S1b (eq 8).

dx.doi.org/10.1021/ed1007712 | J. Chem. Educ. 2012, 89, 1159–1167

other hand, when comparing phenols to indoles (Supporting Information, Figure S1a), one cannot unequivocally rank reaction rates, which vary as a function of cell potential as expected from Marcus Theory. In fact, at a cell potential of about +30 mV, k_2 is roughly the same for all three data sets. Again, this is predicted by Marcus Theory, because ±30 mV marks the edge of the "normal" region.

Second, the notion of the "normal" region is one that escapes some authors. For example, Candeias et al.[28] assumed that a lower reorganization energy always yields a lower activation free energy and a higher rate constant. They concluded erroneously that indoles at pH 7 react more slowly than phenols solely because of the lower A_{ET}/K_d (referred to as k_0/K_m in their paper, ref 28). As discussed above, part of this sluggishness is in fact caused by the 5-fold *lower* reorganization energy at pH 7.

Finally, a word is in order concerning experimental error and uncertainty in nonlinear fitting. Of the four data sets in Figure 9 and Supporting Information, Figure S1 (pH 7 phenols appear in both figures), two do not extend beyond the inverted region, and none contain enough points to clearly define the peak of the k_{ET} vs cell potential curve. This is often a problem in Marcus analyses: the range of cell potentials tested is limited by the reactants that are available. Furthermore, experimental error in kinetic results can be an order of magnitude or more, hence the scatter in data points is often high (for example, see the blue k_2 points between −0.1 and 0.0 V in Figure 9). For these reasons, nonlinear fits using the Marcus Equations can sometimes seem unconvincing, or, as one colleague put it, the fitted lines seem like "wishful thinking." Even so, all of this is recognized and accepted in the peer-reviewed electrochemistry literature. At the same time, I have magnified these fitting "warts" by plotting k vs cell potential. In the literature authors almost always plot $\ln(k)$ vs cell potential, thus minimizing the appearance of scatter. However, the semilog plot underweights the importance of high rates in the fitting process, and overweights the importance of low rates, which can lead to inaccurate fitting results.

Even with this drawback, the $\ln(k)$ vs cell potential semilog plot can serve a useful purpose, especially when the range of available cell potentials is limited and data scatter is substantial. The semilog version of k_2 and k_3 for peroxidase reduction by phenols is shown in Figure 11. As with the k vs cell potential curve, in the semilog plot, λ controls both the shape (width) and the placement along the cell potential axis; A_{ET}/K_d controls placement along the $\ln(k)$ axis. From the fact that the k_2 curve closely resembles the k_3 curve displaced vertically upward (Figure 11), Folkes and Candeias[25] concluded (correctly) that the main difference between the two steps lay not in λ, but in A_{ET}/K_d.

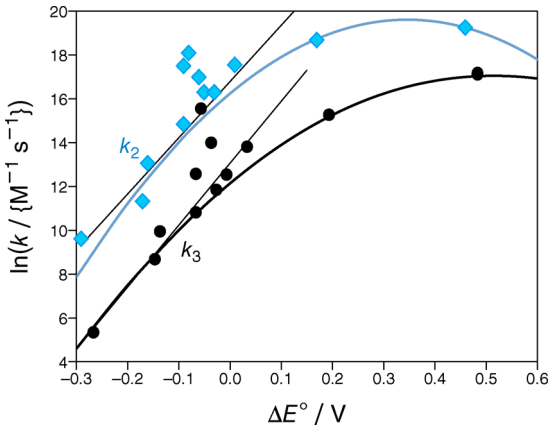

Figure 11. Semilog plot of data in Figure 9, with straight line drawn through first four points: $\ln[k_2, M^{-1} s^{-1}]$), blue diamonds, slope = 26 ± 6 V^{-1}, intercept = 16.8 ± 1.2, R^2 = 0.90; $\ln(k_3, M^{-1} s^{-1})$, black circles, slope = 28 ± 4 V^{-1}, intercept = 13.1 ± 0.7, R^2 = 0.95.

Quantitative results can also be extracted from semilog plots. By differentiating eqs 1 and 2, Marcus showed[5] that small regions of the semilog plot are linear.[46] For the $\ln(k_{ET})$ vs $\Delta G°$ plot, the slope has units of mol/kJ, and is a function of $\Delta G°/\lambda$:

$$-RT \times \text{slope} = \frac{1}{2}(1 + \Delta G°/\lambda) \tag{6}$$

For the $\ln(k_{ET})$ vs $\Delta E°$ plot, the slope has units of V^{-1}, and is a function of $\Delta E°/\lambda$:

$$(RT/F) \times \text{slope} = \frac{1}{2}(1 - \Delta E°/\lambda) \tag{7}$$

Using eq 7, one can obtain a value for λ independent of that derived from nonlinear fitting of the k vs cell potential curve:

$$\lambda = \frac{\Delta E°_{mid}}{[1 - (2RT/F) \times \text{slope}]} \tag{8}$$

where $\Delta E°_{mid}$ is the midpoint of the linear range of cell potentials selected. For the Candeias et al. peroxidase results in Figure 9 and Supporting Information, Figure S1, λ obtained from eq 8 and semilog slopes agrees with that from nonlinear fitting of eq 3 and 5 within ≈10% for three of the four data sets (Table 1). This adds to our confidence in the accuracy of the best-fit parameters derived from these measurements.

Other recent Marcus analyses[30−32] have compared sets of organic reductant substrates (e.g., phenols, phenothiazines, phenylenediamines) interacting with peroxidase and laccase enzymes from various species. In general, differences in rate constants are due either to A_{ET}/K_d alone (as in Figure 9), or to a combination of both λ and A_{ET}/K_d (as in Supporting Information, Figure S1). Rarely, it seems, do changes in λ alone cause a dramatic shift in reaction rate, but Roth and Klinman[33] recently made just such an argument for glucose oxidase. Glucose oxidase works via a "ping pong" mechanism in which the flavoenzyme is first reduced by glucose in a two-electron process (glucose-CHOH + FAD → gluconolactone=O + $FADH:^- + H^+$), and then oxidized by dioxygen in a sequence of two one-electron steps:[47,48]

The first of the steps in Scheme 2, creating the flavosemiquinone and superoxide radicals, is rate-limiting.[33,49,50] Also, the active site $histidine_{516}$ is a critical residue: In the initial enzyme reduction step the deprotonated imidazole side chain on his_{516} base-catalyzes proton removal from glucose's C_1H-OH hydroxyl group;[50] in the subsequent enzyme oxidation step depicted in Scheme 2, the protonated his_{516} group serves a key catalytic function.[33,50] One would ordinarily expect this latter function to involve acid-catalysis, however, the rate-determining step of enzyme oxidation (creation of the flavin and superoxide radicals) involves electron transfer only.

Scheme 2

$$FADH:^- + O_2\ (+H^+) \rightarrow FADH\bullet + O_2\bullet^-\ (+H^+) \rightarrow FAD + H_2O_2$$

dx.doi.org/10.1021/ed1007712 | J. Chem. Educ. 2012, 89, 1159−1167

This and other lines of evidence[51] suggest that the protonated $his_{516}H^+$ optimizes enzyme oxidation/dioxygen reduction via its positive charge rather than its acidity.[33] The importance of establishing a "favorable electrostatic environment" to lower the activation energy of enzyme-catalyzed hydrogen-transfer reactions has recently been discussed.[52] In fact, in their temperature studies of glucose oxidase activity at high pH and low pH, Roth and Klinman[33] showed that the enhanced activity of the low pH form of the enzyme is due to its lower activation energy (3.0 vs 9.0 kcal/mol), and not to any large difference in frequency factor (0.5−4 nM^{-1} s^{-1} at the pH extremes). The authors concluded that the positive charge of the protonated his_{516} imidazole lowered the activation energy for electron transfer from reduced $FADH:^-$ to dioxygen[33] by lowering the reorganization energy of the one-electron transfer reaction. They calculated values of λ = 23 kcal/mol (1.0 eV) at low pH vs 42 kcal/mol (1.8 eV) at high pH. Although the magnitude of this difference may be affected by corrections to calculation errors,[53] the conclusion that the positive charge of $his_{516}H^+$ at the active site serves to aid catalysis by orienting solvent in the active site environment and lowering reorganization energy seems secure. This echoes the effects of low reorganization energies seen for electron transfer within the photosynthetic reaction center.[38]

CONCLUSION

Marcus Theory has been applied usefully to inorganic and biological electron transfer reactions. Generally these analyses are carried out on a set of rate constants for a series of related redox enzyme reactions with differing cell potentials. The series can comprise either a single enzyme reacting with structurally related substrates (e.g., phenols, indoles, phenylenediamines, phenothiazines) or a single substrate reacting with a series of related enzymes. Not all such cell potential, rate constant data sets show the bell-shaped peak expected from Marcus Theory. There are at least five reasons why this might be the case: (1) The redox enzyme-catalyzed reaction is inner-sphere (unusual for enzymes). (2) The rate-determining step is product release rather than electron transfer (i.e., $k_{rel} \ll k_{ET}$);[54,55] in this case, because product release involves nuclear motion, Figure 1 would be a gross oversimplification and there should be no discernible relationship between ΔG° and $\Delta G^\ddagger$. Or, the series of steps in Scheme 1 may feature inconstant (3) binding parameters (k_a, k_{-a}, K_d); (4) binding orientation/electron transfer distance (A_{ET}); or (5) reorganization energy (λ). However, for reactions that *are* successfully described by Marcus Theory, informative comparisons can be made regarding differences in reorganization energy (λ) vs binding (k_a, A_{ET}/k_{-a}, or A_{ET}/K_d). Furthermore, Marcus Theory illustrates two points of interest to upper division chemistry undergraduates: thermodynamics do control kinetics for outer-sphere electron transfer reactions (unlike most other chemical reactions); and the reason for this can be explained with straightforward applications of common physical chemical concepts like transition state theory, Arrhenius' Law, and the Franck−Condon Principle.

ASSOCIATED CONTENT

Supporting Information

Derivation of A_{ET} vs A_0, derivation of the Marcus Equation, and steady state derivation of eq 4, and Figures S1a, S1b, and S2. This material is available via the Internet at http://pubs.acs.org.

AUTHOR INFORMATION

Corresponding Author

*E-mail: tsilvers@willamette.edu.

Present Address

School of Chemistry, National University of Ireland, Galway, Ireland.

Notes

The authors declare no competing financial interest.

ACKNOWLEDGMENTS

I wish to thank my colleagues Donal Leech for his helpful suggestions and encouragement, and J. Charles Williamson, who went above and beyond the call of duty in his close reading and constructive criticisms of this paper.

REFERENCES

(1) Schultz, E. *J. Chem. Educ.* **2010**, *87*, 472−473.

(2) Silbey, R. J.; Alberty, R. A.; Bawendi, M. G. *Physical Chemistry*, 4th ed.; J.Wiley & Sons: New York, 2005; pp 690−692.

(3) In "inner sphere" redox reactions, the donor and acceptor are connected by chemical bonds or bridges, and through-bond electron transfer may occur.

(4) Marcus, R. A. (**1992**) "Rudolph A. Marcus - Nobel Lecture". *Nobelprize.org*. June 24, 2010; http://nobelprize.org/nobel_prizes/chemistry/laureates/1992/marcus-lecture.html.

(5) Marcus, R. A.; Sutin, N. *Biochim. Biophys. Acta* **1985**, *811*, 265−322.

(6) Scott, R. A.; Mauk, A. G.; Gray, H. B. *J. Chem. Educ.* **1985**, *62*, 932−938.

(7) Van Houten, J. *J. Chem. Educ.* **2002**, *79*, 1055−1059.

(8) Martins, L. J. A.; da Costa, J. B. *J. Chem. Educ.* **1988**, *65*, 176−178.

(9) Newton, T. W. *J. Chem. Educ.* **1968**, *45*, 571−575.

(10) Lewis, N. A. *J. Chem. Educ.* **1980**, *58*, 478−483.

(11) Neta, P. *J. Chem. Educ.* **1981**, *79*, 110−113.

(12) For electron transfer at electrodes, either D or A could represent the electrode; for biological electron transfer reactions, either D or A could represent a redox enzyme.

(13) Because of the difference between the Arrhenius activation energy (E_a) and the Eyring activation free energy ($\Delta G^\ddagger$), A_{ET} in eq 1 actually equals the Arrhenius frequency factor (A_0) divided by $e^{(1+\Delta S^\ddagger_{rot}/R)}$ (derivation in Supporting Information A).

(14) Interestingly, β values measured for nonphotochemical adiabatic systems all seem to lie in the 10−15 nm^{-1} (1.0−1.5 $Å^{-1}$) range, with nonbiological reactions[5] centered around 12 ± 2 nm^{-1}, and biological electron transfers closer to 14 ± 2 nm^{-1}. The exponential distance dependence factor, β, can be interpreted roughly in terms of electron tunnelling through a square potential barrier[5,14]; values of β = 11 and 15 nm^{-1} represent barrier heights of 1.1 and 2.1 eV, or 110 and 200 kJ/mol, respectively[5]. For a particular redox reaction, $\kappa(r)$ is assigned an average value of κ over the relevant range of electron transfer distances; for an adiabatic reaction, that is, one with strong electronic coupling between reactants, $\kappa \approx 1$.

(15) Marcus, R. A. *Annu. Rev. Phys. Chem.* **1964**, *15*, 155−196.

(16) The converse works just as well: a single acceptor with a series of related donors.

(17) Candeias, L. P.; Folkes, L. K.; Porssa, M.; Parrick, J.; Wardman, P. *Biochemistry* **1996**, *35*, 102−108.

(18) A simplified derivation of eq 2 is included in the Supporting Information B.

(19) Marcus explains the situation thusly[5]: because of the "small overlap of the electronic orbitals, it then follows that [electron] transfer will occur only at or near nuclear configurations for which the total potential energy of the [solvated] reactants is equal to that of the [solvated] products."

(20) From eq 3, $\Delta G^{\ddagger}(\lambda_{low}) = \Delta G^{\ddagger}(\lambda_{high})$ when $\lambda_{low} = \Delta E^{\circ 2}/\lambda_{high}$. Hence, as long as $\lambda_{low} > \Delta E^{\circ 2}/\lambda_{high}$, $\Delta G^{\ddagger}(\lambda_{low}) < \Delta G^{\ddagger}(\lambda_{high})$ and $k_{ET}(\lambda_{low}) > k_{ET}(\lambda_{high})$, i.e., the behavior assumed by many authors. However, if $\lambda_{low} < \Delta E^{\circ 2}/\lambda_{high}$, the opposite holds true. In other words, if $\Delta E^{\circ} = 1$ eV and $\lambda_{high} = 2$ eV (point *b* in Figure 3), then as long as $0.5 < \lambda_{low} < 2$ eV (point *b*′), $\Delta G^{\ddagger}(\lambda_{low}) < \Delta G^{\ddagger}(\lambda_{high})$. However, if $\lambda_{low} < 0.5$ eV, then $\Delta G^{\ddagger}(\lambda_{low}) > \Delta G^{\ddagger}(\lambda_{high})$. Similar conclusions can be drawn concerning $\lambda_{high} = 4$ eV (point *c* in Figure 3): The cutoff in this case is at $\lambda_{low} = 0.25$ eV (point *c*′).

(21) This is true for the special case of A_{ET} (low λ) = A_{ET} (high λ). If A_{ET} (low λ) ≠ A_{ET} (high λ), then the "normal" range is bounded by $\pm f\sqrt{\lambda_{low}\lambda_{high}}$, where $f = \{1-[4RT/(nF(\lambda_{high} - \lambda_{low})]\ \ln(A_{ET,\lambda_{high}}/A_{ET,\lambda_{low}})\}^{1/2}$.

(22) From eqs 1−3, $\Delta w_{1/2} = 4[\lambda\cdot(-w_{rct} + RT\ \ln(A_{ET}/k_{-a}) + 2\ e^{w_{rct}/RT})/(nF)]^{1/2})$. If binding is rate-limiting (i.e., $k_{-a} \ll A_{ET}$), then this reduces to $\Delta w_{1/2} = 4[\lambda\cdot(-w_{rct} + RT\ \ln(A_{ET}/k_{-a}))/(nF)]^{1/2})$. If electron transfer is rate-limiting (i.e., $k_{-a} \gg A_{ET}$), then this reduces to $\Delta w_{1/2} = 4[\lambda\cdot(RT\ \ln(2))/(nF)]^{1/2})$, which for $n = 1$ and $T = 25$ °C gives $\Delta w_{1/2} = (0.534\ V^{1/2})\sqrt{\lambda}$.

(23) Weaver, M. J. *J. Phys. Chem.* **1980**, *84*, 568−576.

(24) Saveant, J.-M.; Tessier, D. *Faraday Discuss. Chem. Soc.* **1982**, *74*, 57−72.

(25) Folkes, L. K.; Candeias, L. P. *FEBS Lett.* **1997**, *412*, 305−308.

(26) Khopde, S. M.; Priyadarsini, K. I. *Biophys. Chem.* **2000**, *88*, 103−109.

(27) Candeias, L. P.; Folkes, L. K.; Porssa, M.; Parrick, J.; Wardman, P. *Biochemistry* **1996**, *35*, 102−108.

(28) Candeias, L. P.; Folkes, L. K.; Wardman, P. *Biochemistry* **1997**, *36*, 7081−7085.

(29) Kulys, J.; Deussen, H.-J.; Krikstopaitis, K.; Lolke, R.; Schneider, P.; Ziemys, A. *Eur. J. Org. Chem.* **2001**, *2001*, 3475−3484.

(30) Krikstopaitis, K.; Kulys, J.; Pedersen, A. H.; Schneider, P. *Acta Chim. Scand.* **1998**, *52*, 469−474.

(31) Kulys, J.; Krikstopaitis, K.; Ziemys, A. *JBIC* **2000**, *5*, 333−340.

(32) Xu, F. *Biochemistry* **1996**, *35*, 7608−7614.

(33) Roth, J. P.; Klinman, J. P. *Proc. Natl. Acad. Sci. U.S.A.* **2003**, *100*, 62−67.

(34) Forrow, N. J.; Sanghera, G. S.; Walters, S. J. *J. Chem. Soc., Dalton Trans.* **2002**, *2002*, 3187−3194.

(35) Zakeerudin, S. M.; Fraser, D. M.; Nazeerudin, M.-K.; Gratzel, M. *J. Electroanal. Chem.* **1992**, *337*, 253−283.

(36) Zakeerudin, S. M.; Gratzel, M.; Fraser, D. M. *Biosens. Bioelectron.* **1996**, *11*, 305−315.

(37) Zhang, C.; Haruyama, T.; Kobatake, E.; Aizawa, M. *Anal. Chim. Acta* **2000**, *408*, 225−232.

(38) Jia, Y.; DiMagno, T. J.; Chan, C.-K.; Wang, Z.; Du, M.; Hanson, D. K.; Schiffer, M.; Norris, J. R.; Fleming, G. R.; Popov, M. S. *J. Phys. Chem.* **1993**, *97*, 13180−13191.

(39) Penner-Hahn, J. E.; Eble, K. S.; McMurry, T. J.; Renner, M.; Balch, A. L.; Groves, J. T.; Dawson, J. H.; Hodgson, K. O. *J. Am. Chem. Soc.* **1986**, *108*, 7819−7825.

(40) Schultz, C. E.; Devaney, P. W.; Winkler, H.; Debrunner, P. G.; Doan, N.; Chiang, R.; Rutter, R.; Hager, L. P. *FEBS Lett.* **1979**, *103*, 102−105.

(41) Veitch, N. C. *Biochem. Soc. Trans.* **1995**, *23*, 232−239.

(42) For indoles at pH 5 (Supporting Information, Figure S1a), the data could only be fit using the three-parameter fit from eqs 1, 3, and 4, suggesting that binding (not electron transfer) is rate-limiting.

(43) Except at $\Delta E^{\circ} = 0.03\ V \approx \lambda$. Here all three rate constants (k_2 for phenols at pH 7, indoles at pH 7, and indoles at pH 5) are about the same.

(44) This data set could only be fit by assuming that binding (not electron transfer) is rate-limiting. Best-fit results are: $k_a = 38.3 \pm 0.9\ \mu M^{-1}\ s^{-1}$, and $A_{ET}/k_{-a} = 11.1 \pm 1.0$ (unitless); thus $A_{ET}/K_d = k_a(A_{ET}/k_{-a}) = 430 \pm 40\ \mu M^{-1}\ s^{-1}$.

(45) Except at $\Delta E^{\circ} = 0.03\ V \approx \lambda$. Here, saturation due to the rate-limiting binding step keeps the rate constant low.

(46) This is essentially a kinetic Linear Free Energy Relationship applied to electron transfer. It is an application of the Bell−Evans−Polanyi Principle, also known as the Bronsted Catalysis Law (see Roy, S.; Goedecker, S.; Hellmann, V. *Phys. Rev. E* **2008**, *77*, 056707 , and references cited therein).

(47) Gibson, Q. H.; Swoboda, B. E. P.; Massey, V. *J. Biol. Chem.* **1966**, *239*, 3927−3934.

(48) Weibel, M.; Bright, H. J. *J. Biol. Chem.* **1971**, *246*, 2734−2744.

(49) Palfey, B. A.; Ballou, D. P.; and Massey, V. In *Active Oxygen in Biochem-Biochemistry*; Valentine, J. S., Foote, C. S., Greenberg, A., Liebman, J. F., Eds.; Chapman & Hall: New York, 1995; pp 37−83.

(50) Leskovac, V.; Trivic, S.; Wohlfart, G.; Kandrac, J.; Pericin, D. *Int. J. Biochem. Cell Biol.* **2005**, *37*, 731−750.

(51) For example, the kinetic isotope effect is weak, as is the rate dependence on solvent viscosity; also, the kinetic isotope effect is unaltered by pH and unaltered by removal of the imidazole group in the his_{516}→ala_{516} mutant.

(52) Hammes-Schiffer, S.; Benkovic, S. J. *Annu. Rev. Biochem.* **2006**, *75*, 519−541.

(53) After corrections to values of $\Delta G^{\ddagger}$ and w_{rct}, I get λ(low-pH) = 56 kcal/mol vs λ(high-pH) = 66 kcal/mol.

(54) Cleland, W. W. *Acc. Chem. Res.* **1975**, *8*, 145−151.

(55) Cleland[54] argues that for many (perhaps even most) enzymes, product release and not catalysis is rate-limiting. Regarding redox enzymes, he gives evidence that this is the case for a number of dehydrogenases (glyceraldehyde-3-phosphate, alcohol, and lactate, but NOT glutamate) and oxidative decarboxylases (malate and isocitrate).